HHS Public Access

Author manuscript

Neuropharmacology. Author manuscript; available in PMC 2016 October 01.

Published in final edited form as:

Neuropharmacology. 2015 October ; 97: 376–382. doi:10.1016/j.neuropharm.2015.04.009.

Heterologous expression and nonsense suppression provide insights into agonist behavior at α6β2 nicotinic acetylcholine receptors

Michael R. Post[a], **Walrati Limapichat**[a], **Henry A. Lester**[b], and **Dennis A. Dougherty**[a,*]

[a]Division of Chemistry and Chemical Engineering, California Institute of Technology, 1200 E California Blvd., Pasadena, CA 91125, USA

[b]Division of Biology and Biological Engineering, California Institute of Technology, Pasadena, CA, USA

Abstract

The α6-containing subtypes of the nicotinic acetylcholine receptor (nAChR) are localized to presynaptic terminals of the dopaminergic pathways of the central nervous system. Selective ligands for these nAChRs are potentially useful in both Parkinson's disease and addiction. For these and other goals, it is important to distinguish the binding behavior of agonists at the α6-β2 binding site versus other subtypes. To study this problem, we apply nonsense suppression-based non-canonical amino acid mutagenesis. We report a combination of four mutations in α6β2 that yield high-level heterologous expression in *Xenopus* oocytes. By varying mRNA injection ratios, two populations were observed with unique characteristics, likely due to differing stoichiometries. Responses to nine known nAChR agonists were analyzed at the receptor, and their corresponding EC_{50} values and efficacies are reported. The system is compatible with nonsense suppression, allowing structure–function studies between Trp149 – a conserved residue on loop B found to make a cation-π interaction at several nAChR subtypes – and several agonists. These studies reveal that acetylcholine forms a strong cation-π interaction with the conserved tryptophan, while nicotine and TC299423 do not, suggesting a unique pharmacology for the α6β2 nAChR.

Keywords

Parkinson's disease; Addiction; Ion channels; Nicotinic acetylcholine receptors; Electrophysiology; Non-canonical amino acids

1. Introduction

The nicotinic acetylcholine receptors (nAChR) are a type of pentameric ligand gated ion channel activated by the neurotransmitter acetylcholine, as well as nicotine and a wide array of related small molecules (Smart and Paoletti, 2012). In addition to its role at the

*Corresponding author. dadougherty@caltech.edu (D.A. Dougherty).

Appendix A. Supplementary data

Supplementary data related to this article can be found at http://dx.doi.org/10.1016/j.neuropharm.2015.04.009.

neuromuscular junction, the neuronal nAChRs are widely distributed throughout the CNS. To date, twelve different subunits of the neuronal nAChR have been identified, α2–α10, and β2–β4 (Le Novère et al., 2002). These subunits assemble in various patterns to form different subtypes with distinct localizations, pharmacological characteristics, and functions in the nervous system (Gotti et al., 2006; Zoli et al., 2014). The most commonly and widely expressed neuronal nAChRs in the brain are the α4β2 and α7 subtypes, and these have been studied in depth (Holladay et al., 1997).

The α6 subunit, which is primarily localized to the ventral tegmental area and substantia nigra pars compacta, is thought to form α6β2 pentamers as well as complex subtypes with three or more different subunits, such as α6α4β2, α6β2β3, and α6α4β2β3 (Gotti et al., 2006; Grady et al., 2010; Gerzanich et al.,1997). In some regions, such as the locus coerulus, α6β4 nAChRs also form (Azam et al., 2010). Subtypes of nAChRs containing the α6 subunit have been of recent interest, as they are found in dopaminergic pre-synaptic terminals and thus influence the release of dopamine in both the nigrostriatal and mesocorticolimbic pathways (Holladay et al., 1997; Quik and Wonnacott, 2011; Quik and McIntosh, 2006; Yang et al., 2009). As such, finding agonists that are selective at these subtypes, specifically the α6-β2 binding site, could be important in studies of both Parkinson's disease and addiction.

A number of structural features are well established for nAChRs. Each subunit has an N-terminal extracellular ligand-binding domain followed by four transmembrane helices, M1–M4 (Miyazawa et al., 2003). Of note are the M2 helix, which lines the channel pore, (Jha et al., 2009) and the intracellular M3–M4 loop, which is thought to be involved in the trafficking of the receptor from the endoplasmic reticulum (ER) to the membrane surface (Kracun et al., 2008). At the interface of two adjacent subunits in the extracellular domain is the ligand binding site, comprised of six loops. Loops A–C are contributed by the primary (α) subunit and D–F by the complementary (β) subunit (Corringer et al., 2000). These loops contribute five conserved residues – TyrA (α6:Y93), TrpB (α6:W149), TyrC1 (α6:Y190), TyrC2 (α6:Y197), and TrpD (β2:W57) – that form an aromatic box responsible for binding the cationic moiety of agonists and antagonists. Previous studies have shown that TrpB in the α4-β2 interface and TyrC2 in the α7–α7 interface make a cation-π interaction with acetylcholine (Van Arnam and Dougherty, 2014). These results contributed to a pharmacophore model of the α4β2 and α7 subtypes and advanced our understanding of the differences in pharmacology among nAChR subtypes.

Various derivatives of α-conotoxins, disulfide-rich peptide antagonists of nAChRs, provide selective antagonism among α6-containing nAChRs (Azam et al., 2010; Hone et al., 2013, 2012). These selective antagonists have provided rich information about the roles of α6-containing subtypes in physiology and behavior. It is thought that additional information can be gained, and perhaps useful drugs found, among selective agonists. However developing agonists selective for α6-containing subtypes requires a deeper understanding of the ligand site, specifically how the α6-β2 binding site differs from those previously studied.

High precision studies of agonist binding in the α4β2 and α7 receptors have utilized nonsense suppression-based non-canonical amino acid mutagenesis in a *Xenopus laevis* oocyte expression system (Dougherty and Van Arnam, 2014). Nonsense suppression is,

however, relatively inefficient, with agonist-induced currents roughly an order of magnitude lower than produced by conventional mutagenesis, making previously reported α6-expression systems such as chimeric subunits, and concatenated subunits unsuitable for this technique (Yang et al., 2009; Kuryatov et al., 2000; Letchworth and Whiteaker, 2011; Wang et al., 2014; Papke et al., 2008; Capelli et al., 2011; Kuryatov and Lindstrom, 2011; Ley et al., 2014). Here, we report a combination of four mutations that result in the controlled and consistent expression of α6β2 at the high levels that permit nonsense suppression and thus incorporation of non-canonical amino acids. Results from such experiments allow preliminary development of a binding model for agonists at α6β2-containing nAChRs.

2. Materials and methods

2.1. Molecular biology

Rat α6 and β2 nAChRs were in the pGEMhe vector. Site-directed mutagenesis was performed using the Stratagene Quik Change protocol. Circular cDNA was linearized with SbfI (New England Biolabs, Ipswich, MA). After purification (Qiagen, Valencia, CA), linearized DNA was used as a template for runoff *in vitro* transcription using T7 mMessage mMachine kit (Life Technologies, Santa Clara, CA). The resulting mRNA was purified (RNAeasy Mini Kit; Qiagen) and quantified by UV spectroscopy.

2.2. Ion channel expression

X. laevis oocytes (stage V to VI) were sourced from both the Caltech facility and Ecocyte Bio Science (Austin, TX). For expression of conventionally mutated nAChRs, oocytes were injected with 50 nL solution containing either 5 or 10 ng mRNA. The α6 to β2 ratio is reported as mass ratio. Cells were incubated for 24–48 h at 18 °C in ND96 solution (96 mM NaCl, 2 mM KCl, 1 mM $MgCl_2$, and 5 mM HEPES, pH 7.5) with 0.005% (w/v) gentamycin and 2% (v/v) horse serum.

2.3. Non-canonical amino acid incorporation

The nitroveratryloxycarbonyl (NVOC) protected cyanomethylester forms of non-canonical amino acids were synthesized, coupled to the dinucleotide dCA, and enzymatically ligated to UAG-suppressor 74-mer THG73 $tRNA_{CUA}$ as previously described (Dougherty and Van Arnam, 2014). The product was verified by MALDI time-of-flight mass spectrometry on a 3-hydroxypicolinic acid matrix. The non-canonical amino acid-conjugated tRNA was deprotected by photolysis on a 500 W Hg/Xe arc lamp, filtered with Schott WG-320 and UG-11 filters, immediately prior to coinjection with mRNA containing the UAG mutation at TrpB. mRNA and tRNA were typically injected in a 1:1 or 1:2 volume ratio in a total volume of 50 or 75 nL respectively so that 25 ng of mRNA was injected per cell. In cases where observed currents were low after 48 h incubation – likely due to low receptor protein expression – a second injection of mRNA and tRNA was performed after 24 h.

The fidelity of non-canonical amino acid incorporation was confirmed at each site with a wild-type recovery experiment by charging tRNA with the wild-type residue. If this experiment yielded similar results to wild type, then aminoacylated tRNA incorporated the non-canonical amino acid and nothing else. A read-through/reaminoacylation test served as

a negative control by injecting unacylated 76-mer tRNA. Lack of current proved no detectable reaminoacylation at the TrpB site.

2.4. Whole-cell electrophysiological characterization

Acetylcholine chloride, choline chloride, carbamylcholine chloride, cytisine, and (−)-nicotine tartrate were purchased from Sigma Aldrich (St Louis, MO), (±)-epibatidine was purchased from Tocris (Bristol, UK), while varenicline (Pfizer) and metanicotine and TC299423 (Targacept) were generous gifts. Agonist-induced currents were recorded in TEVC mode using the OpusXpress 6000A (Molecular Devices, Sunnyvale, CA) at a holding potential of −60 mV. Agonists were prepared in Ca^{2+}-free ND96 and 1 mL was applied for 15 s followed by a 2 min wash using buffer, except epibatidine, which was followed by a five minute wash. Data from dose–response experiments were normalized and averages were fit to the Hill equation, $I_{norm} = 1/(1 + (EC_{50}/[agonist])^{nH})$ where EC_{50} is the effective concentration to activate 50% of the surface receptors, and n_H is the Hill coefficient.

3. Results and discussion

3.1. High-level heterologous expression of α6β2 in Xenopus oocytes

Heterologous expression of α6-containing nAChRs in *Xenopus* oocytes has long posed a challenge in studying these receptors, especially for nonsense suppression. In the present work, four mutations that have been previously been shown to enhance expression in other systems are combined in a strategy that produces functional receptors in oocytes. The first mutation is an L9′S mutation in the M2 helix of the α6 subunit. This mutation is analogous to an L9′A mutation in α4 that has been shown to increase expression and conductance, producing enhanced currents without affecting the pharmacological characteristics of the receptor (Gleitsman et al., 2009; Filatov and White, 1995; Fonck et al., 2005). However, unlike in studies of α4β2, the α6L9′S mutation alone was not enough to produce observable currents in oocytes, as demonstrated in Fig. 1A.

The M3–M4 loop in the β2 subunit is unusual – not only does it have an ER retention motif (RRQR) that is absent in other beta-like subunits, it also lacks a conserved ER export motif (LXM). Eliminating the retention motif and reconstituting the export motif has been shown previously to increase expression of fluorescent protein analogs of α4β2 and α6β2 in a mammalian cell line (Xiao et al., 2011; Srinivasan et al., 2011). Therefore, the mutations 325LFL/LFM327 and 339RRQR/AAQA343 were incorporated into the β2 subunit, and $α6L9′Sβ2_{LFM/AAQA}$ was expressed in oocytes. This modified receptor produced observable currents when exposed to acetylcholine (Fig. 1B).

The waveforms produced by applying a dose of acetylcholine to $α6L9′Sβ2_{LFM/AAQA}$ show opening of the receptor followed by a quick partial closing and a sustained current until agonist washout. The current shape, as well as dose-response curves generated from $α6L9′Sβ2_{LFM/AAQA}$, are inconsistent from cell to cell and typically biphasic or multiphasic, suggesting that multiple populations exist. The inconsistent results from this subtype along with an average maximum current of only 0.25 μA make $α6L9′Sβ2_{LFM/AAQA}$ unsuitable for non-canonical amino acid mutagenesis.

In order to further increase expression levels, an L9′S mutation was added to the β2 subunit. The resulting α6L9′Sβ2L9′$S_{LFM/AAQA}$ construct was injected into oocytes and yielded currents consistently greater than 1 μA in response to acetylcholine, as in Fig. 1C. The current traces were consistent from cell to cell and showed a sustained channel opening until agonist washout. Dose response curves generated from α6L9′Sβ2L9′$S_{LFM/AAQA}$ were monophasic, with consistent EC_{50} measurements. Previous work on the mouse-muscle type nAChR showed leak currents to be too high to produce consistent results when all five subunits contained an L9′S mutation; however, the α6L9′Sβ2L9′$S_{LFM/AAQA}$ receptor (combined mutations will be indicated by α6β2‡ from here on) consistently produced baseline current levels much less than the observed maximum current due to agonist activation.

3.2. Stoichiometry control of α6β2‡ in oocytes

As part of an effort to optimize expression of α6β2‡ in oocytes, the mRNA injection ratio of α6 to β2 was varied. Ratios from 50:1 to 1:20 were used while keeping the total amount of mRNA constant at 10 ng in each cell. Two different phenotypes were observed based on mRNA injection ratio, as seen in Fig. 2 and Table 1: an α6-biased population that had an EC_{50} of about 0.11 μM and a Hill coefficient greater than 1, and a β2-biased population that had an EC_{50} around 0.5 μM and a Hill coefficient less than 1. A general attenuation in maximum currents was also observed in the β2-biased population, although this is difficult to quantify because of natural variations in maximum currents due to oocyte variability.

The different phenotypes observed likely result from a difference in subunit stoichiometries based on the mRNA ratio; that is, when more α6 mRNA is injected than β2 mRNA, more alpha subunits will be translated, and they will pentamerize in a combination with more alpha subunits than beta subunits. The tight distribution of EC_{50} values and Hill coefficients suggests a single stoichiometry is activated in the α6-biased injection ratios, while low Hill coefficients and high variation in EC_{50} values in the β2-biased ratios suggests a mixture of stoichiometries is present. This mRNA injection ratio effect is similar to what has been observed throughout the literature with α4β2 nAChRs, where two stoichiometries have been confirmed – $(\alpha4)_3(\beta2)_2$ and $(\alpha4)_2(\beta2)_3$ (Nelson et al., 2003; Moroni et al., 2006). Because it is better behaved, the α6-biased population will be used in binding studies conducted in this report.

3.3. Agonists at α6β2‡

With a controlled and uniform population of α6β2‡ receptors expressed in *Xenopus* oocytes now available, a panel of agonists was screened. The nAChR agonists acetylcholine, nicotine, meta-nicotine, varenicline, cytisine, choline, carbamylcholine, and epibatidine were evaluated. We also considered TC299423, a modestly α6β2 subtype-selective agonist that can serve as a probe for involvement of this subtype in α6-mediated behaviors (structures shown in Fig. 3) (Wall, 2015). As shown in Table 2, metanicotine, choline and carbamylcholine are less potent than ACh. Nicotine, varenicline, cytisine, and TC299423 are slightly more potent, and epibatidine has an EC_{50} several orders of magnitude lower than ACh. These trends are consistent with chimeric α6β2 expression systems previously reported where nicotine had a lower EC_{50} than acetylcholine (Wang et al., 2014). Relative

efficacy experiments were conducted by applying acetylcholine, followed by a dose of agonist sufficient to produce the maximum current in dose response experiments, and then a second application of acetylcholine, with wash-out steps in between. No difference in current between the first and second applications of ACh was seen; that is, no agonist demonstrated desensitization after wash-out. The efficacy values in Table 2, determined by dividing agonist-induced current by ACh-induced current, show these molecules act as partial agonists to varying degrees.

3.4. Non-canonical amino acids: ACh at TrpB

To establish the viability of this expression system and as a preliminary evaluation of the α6β2 agonist binding site, we tested the feasibility of using the nonsense suppression methodology for incorporating non-canonical amino acids into α6β2‡ receptors. As noted, nonsense suppression is an inefficient process, resulting in lower yields of the subunit that is the target of non-canonical amino acid incorporation. This could lead to altered stoichiometries or other complications in evaluating the agonist binding site.

Because TrpB has been shown to form a cation-π interaction in many other nAChRs (Van Arnam and Dougherty, 2014), this was the first residue probed using non-canonical amino acid mutagenesis in α6β2‡. The general strategy to probe for a cation-π interaction at a tryptophan employs structure–function studies, wherein the interaction is incrementally weakened with the addition of fluorine atoms to the indole ring side chain. As the electron density is withdrawn from the ring, the interaction is weakened, and an increase in EC_{50} is observed. If a cation-π interaction is present between an agonist and TrpB, a linear correlation will exist between the log fold-shift in EC_{50} for a given fluorinated tryptophan and the calculated binding energy between a prototype cation and that fluorinated tryptophan.

For initial nonsense suppression experiments, a 10:1 mRNA ratio was employed for α6β2‡. Considering first the fold-shifts in ACh EC_{50} of 5-F_1Trp, 5,7-F_2Trp, and 5,6,7-F_3Trp relative to Trp, there is a clear trend (Table 3). To be certain this correlation was due to electronic effects, we compared three residues with a single substitution, all at the 5 position of the indole ring: 5-F-Trp, 5-Me-Trp and 5-Br-Trp. The steric demands of these substituents are Br > Me > F, while the cation-π modifying ability is F ≈ Br > Me. The data follow the cation-π prediction well, and cannot be interpreted as a steric effect. Fig. 4 shows all the data collected at TrpB. There are some outliers in the analysis. While 5-F-Trp and 6-F-Trp show very similar results (as expected), 4-F-Trp is 3–4-fold more potent than expected, producing near wild type behavior. This is the only non-canonical amino acid we studied with a substituent in the 4 position, suggesting a special interaction at this site. Also, a 5-CN substituent, which is predicted to be strongly inactivating, shows the expected loss of function, but the effect is roughly 5-times greater than predicted. Taken as a whole, however, these results provide strong evidence that ACh is involved in a cation-π interaction with TrpB in the α6 subunit (Table 4).

As noted above, experiments involving non-canonical amino acid mutagenesis might alter the stoichiometry of the receptor being expressed. Therefore, non-canonical amino acid studies were done for a range of mRNA ratios. As shown in Fig. 5, the results from all three

ratios are consistent with each other. The fluorination plots have linear fits, and the Hill coefficients remain significantly >1. Nonsense suppression was attempted at β-biased mRNA ratios, but no currents were observed. We are thus confident that the nonsense suppression experiments are evaluating the same receptor stoichiometry as in the wild type experiments.

3.5. Nicotine and TC299423

The same strategy was used to evaluate whether nicotine and TC299423 make cation-π interactions at TrpB (Fig. 6). For nicotine, mono-substituted Trp residues show the expected shifts in EC_{50}, but F_2-Trp and F_3-Trp are not meaningfully different from F_1-Trp. This rules out a strong cation-π interaction. A more complicated result is seen with TC299423, but again, the results do not support the formation of a strong cation-π interaction. Recall that these exact side chain modifications were employed with ACh and produced a clear linear response, showing that the receptor can readily accommodate these modest structural changes. We cannot rule out a weak interaction between these agonists and TrpB, but the hallmark cation-π interaction seen in many Cys-loop receptors is clearly absent.

Prior to this work, we have performed fluorination studies of the sort described here for 26 different combinations of drug and pentameric receptor (Dougherty and Van Arnam, 2014). In 22 of those cases, a cation-π interaction was found at an aromatic residue that aligns with TrpB. This includes the α4β2 nAChR, which is thought to play a prominent role in nicotine addiction, where both ACh and nicotine display a strong cation-π interaction to TrpB. The pattern seen here in $\alpha6\beta2^{\ddagger}$ receptors, however, is reminiscent of that seen in the muscle-type nAChR, where ACh does but nicotine does not make a cation-π interaction (Beene et al., 2002). The difference between muscle-type and α4β2 was explained by the residue at the i + 4 position relative to TrpB (shown in Fig. 7); a lysine in the α4 subunit, but a glycine in α1 (muscle-type) (Puskar et al., 2012; Xiu et al., 2009). However, the aligned residue is a lysine in α6, indicating the need for a different explanation. Note also that nicotine is not very potent at the muscle-type receptor, but it is more potent than ACh at $\alpha6\beta2^{\ddagger}$, further highlighting the unique nature of α6-containing receptors. It thus appears that the α6β2 nAChR presents a distinctive agonist binding site, and further detailed studies will be required to fully characterize it.

4. Conclusions

The combination of α6L9′S and $\beta2L9'S_{LFM/AAQA}$ subunits in the $\alpha6\beta2^{\ddagger}$ construct produces enough current to permit nonsense suppression, allowing structure–function studies of the binding site at the α6-β2 interface. In these first studies, we have found that ACh makes a cation-π interaction to TrpB, as is often seen. Interestingly, nicotine and TC299423 do not make a comparable cationπ interaction. This suggests the potential for interesting and novel pharmacology for α6-containing nAChRs.

Supplementary Material

Refer to Web version on PubMed Central for supplementary material.

Acknowledgment

We thank the NIH (NS 34407) for support of this work. MRP was supported by an NIH/NRSA training grant: 5 T32 GM07616.

References

Azam L, Maskos U, Changeux J-P, Dowell CD, Christensen S, De Biasi M, McIntosh JM. α-Conotoxin BuIA[T5A;P6O]: a novel ligand that discriminates between 6 4 and 6 2 nicotinic acetylcholine receptors and blocks nicotine-stimulated norepinephrine release. FASEB J. 2010; 24(12):5113–5123. http://dx.doi.org/10.1096/fj.10-166272. [PubMed: 20739611]

Beene DL, Brandt GS, Zhong W, Zacharias NM, Lester HA, Dougherty DA. Cation–π interactions in ligand recognition by serotonergic (5-HT3A) and nicotinic acetylcholine Receptors: the anomalous binding properties of nicotiney. Biochemistry (Mosc.). 2002; 41(32):10262–10269. http://dx.doi.org/10.1021/bi020266d.

Capelli AM, Castelletti L, Chen YH, Van der Keyl H, Pucci L, Oliosi B, Salvagno C, Bertani B, Gotti C, Powell A, et al. Stable expression and functional characterization of a human nicotinic acetylcholine receptor with α6β2 properties: discovery of selective antagonists. Br. J. Pharmacol. 2011; 163(2):313–329. http://dx.doi.org/10.1111/j.1476-5381.2011.01213.x. [PubMed: 21232042]

Corringer P-J, Novère NL, Changeux J-P. Nicotinic receptors at the amino acid level. Annu. Rev. Pharmacol. Toxicol. 2000; 40(1):431–458. http://dx.doi.org/10.1146/annurev.pharmtox.40.1.431. [PubMed: 10836143]

Dougherty DA, Van Arnam EB. Vivo incorporation of non-canonical amino acids by using the chemical aminoacylation strategy: a broadly applicable mechanistic tool. Chem Bio Chem. 2014; 15(12):1710–1720. http://dx.doi.org/10.1002/cbic.201402080.

Filatov GN, White MM. The role of conserved leucines in the M2 domain of the acetylcholine receptor in channel gating. Mol. Pharmacol. 1995; 48(3):379–384. [PubMed: 7565616]

Fonck C, Cohen BN, Nashmi R, Whiteaker P, Wagenaar DA, Rodrigues-Pinguet N, Deshpande P, McKinney S, Kwoh S, Munoz J, et al. Novel seizure phenotype and sleep disruptions in knock-in mice with hypersensitive α4* nicotinic receptors. J. Neurosci. 2005; 25(49):11396–11411. http://dx.doi.org/10.1523/JNEUROSCI.3597-05.2005. [PubMed: 16339034]

Gerzanich V, Kuryatov A, Anand R, Lindstrom J. "Orphan" α6 nicotinic AChR subunit can form a functional heteromeric acetylcholine receptor. Mol. Pharmacol. 1997; 51(2):320–327. http://dx.doi.org/10.1124/mol.51.2.320. [PubMed: 9203638]

Gleitsman KR, Shanata JAP, Frazier SJ, Lester HA, Dougherty DA. Long-range coupling in an allosteric receptor revealed by mutant cycle analysis. Biophys. J. 2009; 96(8):3168–3178. http://dx.doi.org/10.1016/j.bpj.2008.12.3949. [PubMed: 19383461]

Gotti C, Zoli M, Clementi F. Brain nicotinic acetylcholine receptors: native subtypes and their relevance. Trends Pharmacol. Sci. 2006; 27(9):482–491. http://dx.doi.org/10.1016/j.tips.2006.07.004. [PubMed: 16876883]

Grady SR, Drenan RM, Breining SR, Yohannes D, Wageman CR, Fedorov NB, McKinney S, Whiteaker P, Bencherif M, Lester HA, et al. Structural differences determine the relative selectivity of nicotinic compounds for native α4β2*-, α6β2*-, α3β4*- and α7-nicotine acetylcholine receptors. Neuropharmacology. 2010; 58(7):1054–1066. http://dx.doi.org/10.1016/j.neuropharm.2010.01.013. [PubMed: 20114055]

Holladay MW, Dart MJ, Lynch JK. Neuronal nicotinic acetylcholine receptors as targets for drug discovery. J. Med. Chem. 1997; 40(26):4169–4194. http://dx.doi.org/10.1021/jm970377o. [PubMed: 9435889]

Hone AJ, Scadden M, Gajewiak J, Christensen S, Lindstrom J, McIntosh JM. α-Conotoxin PeIA[S9H, V10A, E14N] potently and selectively blocks 6 2 3 versus 6 4 nicotinic acetylcholine receptors. Mol. Pharmacol. 2012; 82(5):972–982. http://dx.doi.org/10.1124/mol.112.080853. [PubMed: 22914547]

Hone AJ, Ruiz M, Scadden M, Christensen S, Gajewiak J, Azam L, McIntosh JM. Positional scanning mutagenesis of -Conotoxin PeIA identifies critical residues that confer potency and selectivity for

6/3 2 3 and 3 2 nicotinic acetylcholine receptors. J. Biol. Chem. 2013; 288(35):25428–25439. http://dx.doi.org/10.1074/jbc.M113.482059. [PubMed: 23846688]

Jha A, Purohit P, Auerbach A. Energy and structure of the M2 Helix in acetylcholine receptor-channel gating. Biophys. J. 2009; 96(10):4075–4084. http://dx.doi.org/10.1016/j.bpj.2009.02.030. [PubMed: 19450479]

Kracun S, Harkness PC, Gibb AJ, Millar NS. Influence of the M3–M4 intracellular domain upon nicotinic acetylcholine receptor assembly, targeting and function. Br. J. Pharmacol. 2008; 153(7): 1474–1484. http://dx.doi.org/10.1038/sj.bjp.0707676. [PubMed: 18204482]

Kuryatov A, Lindstrom J. Expression of functional human α6β2β3* acetylcholine receptors in Xenopus laevis oocytes achieved through subunit chimeras and concatamers. Mol. Pharmacol. 2011; 79(1):126–140. http://dx.doi.org/10.1124/mol.110.066159. [PubMed: 20923852]

Kuryatov A, Olale F, Cooper J, Choi C, Lindstrom J. Human α6 AChR subtypes: subunit composition, assembly, and pharmacological responses. Neuropharmacology. 2000; 39(13):2570–2590. http://dx.doi.org/10.1016/S0028-3908(00)00144-1. [PubMed: 11044728]

Le Novère N, Corringer P-J, Changeux J-P. The diversity of subunit composition in nAChRs: evolutionary origins, physiologic and pharmacologic consequences. J. Neurobiol. 2002; 53(4): 447–456. http://dx.doi.org/10.1002/neu.10153. [PubMed: 12436412]

Letchworth SR, Whiteaker P. Progress and challenges in the study of α6-containing nicotinic acetylcholine receptors. Biochem. Pharmacol. 2011; 82(8):862–872. http://dx.doi.org/10.1016/j.bcp.2011.06.022. [PubMed: 21736871]

Ley CK-K, Kuryatov A, Wang J, Lindstrom JM. Efficient expression of functional (α6β2)2β3 AChRs in Xenopus oocytes from free subunits using slightly modified α6 subunits. PLoS One. 2014; 9(7):e103244. http://dx.doi.org/10.1371/journal.pone.0103244. [PubMed: 25068303]

Miyazawa A, Fujiyoshi Y, Unwin N. Structure and gating mechanism of the acetylcholine receptor pore. Nature. 2003; 423(6943):949–955. http://dx.doi.org/10.1038/nature01748. [PubMed: 12827192]

Moroni M, Zwart R, Sher E, Cassels BK, Bermudez I. α4β2 nicotinic receptors with high and low acetylcholine sensitivity: pharmacology, stoichiometry, and sensitivity to long-term exposure to nicotine. Mol. Pharmacol. 2006; 70(2):755–768. http://dx.doi.org/10.1124/mol.106.023044. [PubMed: 16720757]

Nelson ME, Kuryatov A, Choi CH, Zhou Y, Lindstrom J. Alternate stoichiometries of α4β2 nicotinic acetylcholine receptors. Mol. Pharmacol. 2003; 63(2):332–341. http://dx.doi.org/10.1124/mol.63.2.332. [PubMed: 12527804]

Papke RL, Dwoskin LP, Crooks PA, Zheng G, Zhang Z, McIntosh JM, Stokes C. Extending the analysis of nicotinic receptor antagonists with the study of α6 nicotinic receptor subunit chimeras. Neuropharmacology. 2008; 54(8):1189–1200. http://dx.doi.org/10.1016/j.neuropharm.2008.03.010. [PubMed: 18448138]

Puskar NL, Lester HA, Dougherty DA. Probing the effects of residues located outside the agonist binding site on drug-receptor selectivity in the nicotinic receptor. ACS Chem. Biol. 2012; 7(5): 841–846. http://dx.doi.org/10.1021/cb200448j. [PubMed: 22296725]

Quik M, McIntosh JM. Striatal α6* nicotinic acetylcholine receptors: potential targets for Parkinson's disease therapy. J. Pharmacol. Exp. Ther. 2006; 316(2):481–489. http://dx.doi.org/10.1124/jpet.105.094375. [PubMed: 16210393]

Quik M, Wonnacott S. α6β2* and α4β2* nicotinic acetylcholine receptors as drug targets for Parkinson's disease. Pharmacol. Rev. 2011; 63(4):938–966. http://dx.doi.org/10.1124/pr.110.003269. [PubMed: 21969327]

Smart TG, Paoletti P. Synaptic neurotransmitter-gated receptors. Cold Spring Harb. Perspect. Biol. 2012; 4(3):a009662. http://dx.doi.org/10.1101/cshperspect.a009662. [PubMed: 22233560]

Srinivasan R, Pantoja R, Moss FJ, Mackey EDW, Son CD, Miwa J, Lester HA. Nicotine up-regulates α4β2 nicotinic receptors and ER exit sites via stoichiometry-dependent chaperoning. J. Gen. Physiol. 2011; 137(1):59–79. http://dx.doi.org/10.1085/jgp.201010532. [PubMed: 21187334]

Van Arnam EB, Dougherty DA. Functional probes of drug–receptor interactions implicated by structural studies: Cys-loop receptors provide a fertile testing ground. J. Med. Chem. 2014; 57(15): 6289–6300. http://dx.doi.org/10.1021/jm500023m. [PubMed: 24568098]

Wall, TR. Effects of TI-299423 on Neuronal Nicotinic Acetylcholine Receptors. Pasadena, CA: California Institute of Technology; 2015.

Wang J, Kuryatov A, Lindstrom J. Expression of cloned α6* nicotinic acetylcholine receptors. Neuropharmacology. 2014 http://dx.doi.org/10.1016/j.neuropharm.2014.10.009.

Xiao C, Srinivasan R, Drenan RM, Mackey EDW, McIntosh JM, Lester HA. Characterizing functional α6β2 nicotinic acetylcholine receptors in vitro: mutant β2 subunits improve membrane expression, and fluorescent proteins reveal responsive cells. Biochem. Pharmacol. 2011; 82(8):852–861. http://dx.doi.org/10.1016/j.bcp.2011.05.005. [PubMed: 21609715]

Xiu X, Puskar NL, Shanata JAP, Lester HA, Dougherty DA. Nicotine binding to brain receptors requires a strong cation–π interaction. Nature. 2009; 458(7237):534–537. http://dx.doi.org/10.1038/nature07768. [PubMed: 19252481]

Yang K, Jin G, Wu J. Mysterious α6-containing nAChRs: function, pharmacology, and pathophysiology. Acta Pharmacol. Sin. 2009; 30(6):740–751. http://dx.doi.org/10.1038/aps.2009.63. [PubMed: 19498417]

Zoli M, Pistillo F, Gotti C. Diversity of native nicotinic receptor subtypes in mammalian brain. Neuropharmacology. 2014 http://dx.doi.org/10.1016/j.neuropharm.2014.11.003.

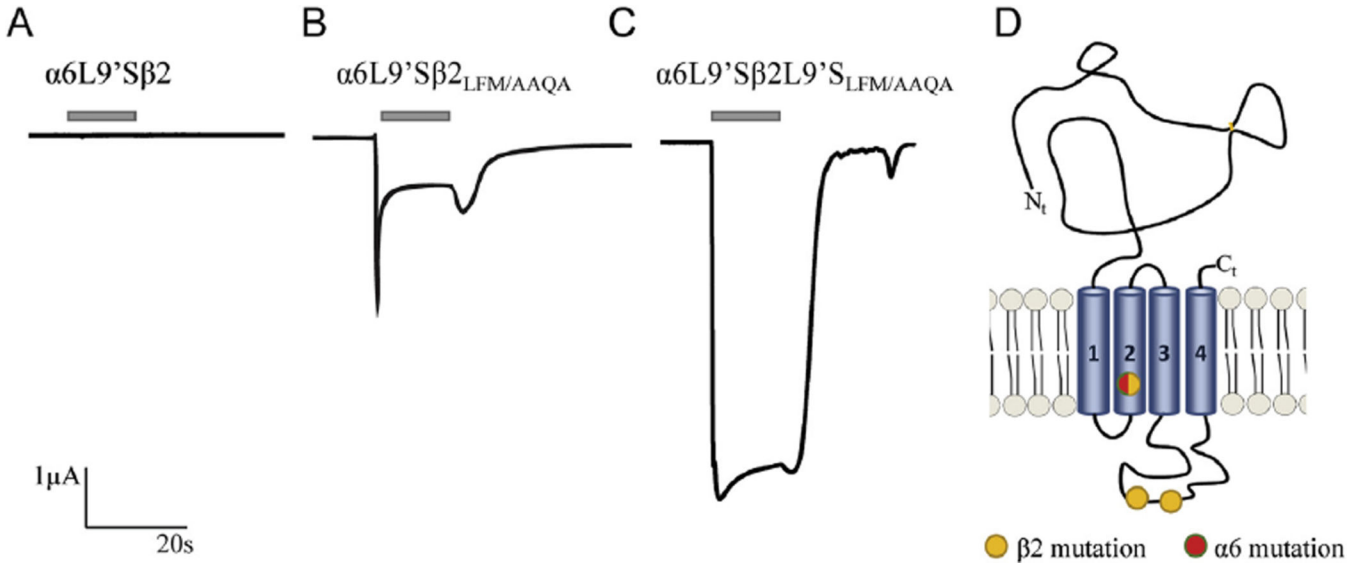

Fig. 1.

Traces of voltage clamp currents showing responses to ACh (A) α6L9′Sβ2, (B) $\alpha 6L9'S\beta 2_{LFM/AAQA}$, (C) $\alpha 6\beta 2^{\ddagger}$, with the mutations shown graphically in (D).

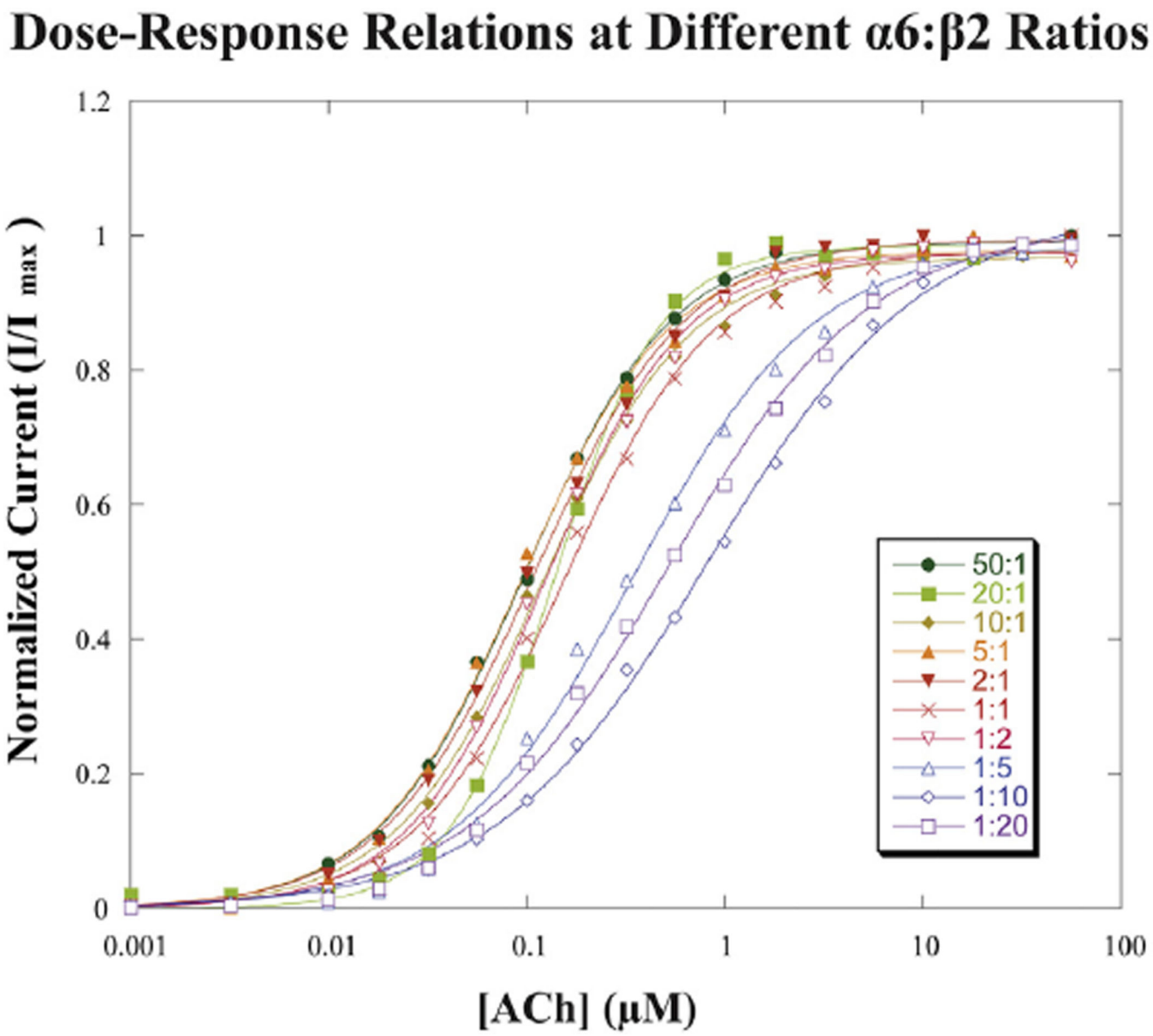

Fig. 2.

Dose–response relationships of α6β2‡ with varying α6:β2 mRNA injection ratios show two distinct populations likely due to differing subunit stoichiometries.

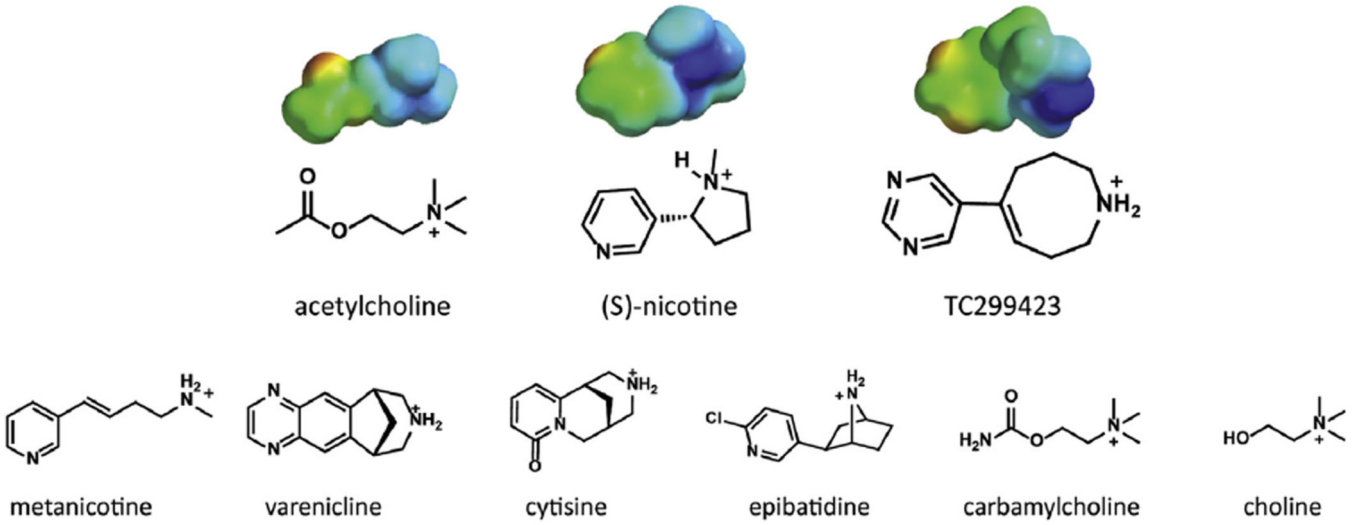

Fig. 3.

Structures of all the agonists studied in this report. Electrostatic potential maps of the agonists involved in structure–function studies were made from HF 6-31G** calculations ranging from −10 (red) to +150 (blue) kcal/mol.

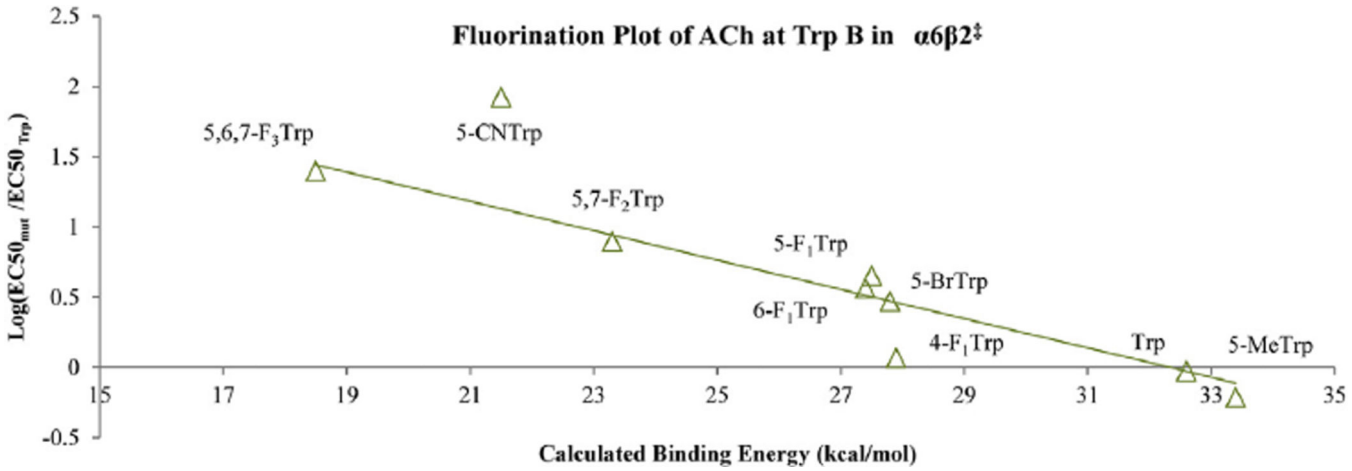

Fig. 4.

Fluorination plot of ACh at TrpB in 10:1 α6β2‡. Linear trend excludes 5-CNTrp and 4-F_1Trp and has a slope of −0.10 which indicates the presence of a strong cation-π interaction between the indole side chain and the cationic agonist.

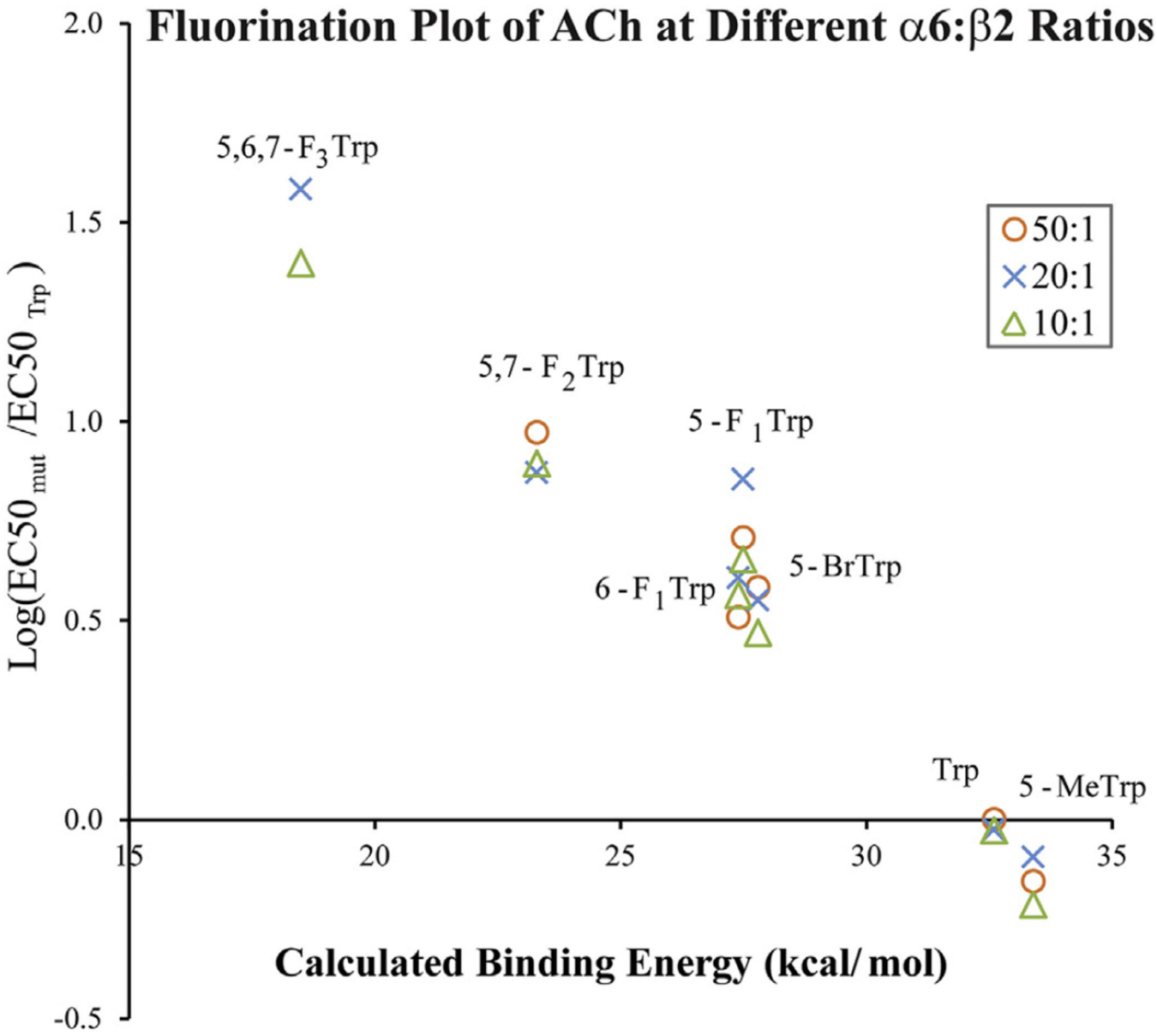

Fig. 5.

Fluorination plot of ACh at Trp B for α6:β2 mRNA injection ratios of 10:1, 20:1, and 50:1. Data are consistent among ratios, confirming that these effects are due to electronics rather than a shift in stoichiometry.

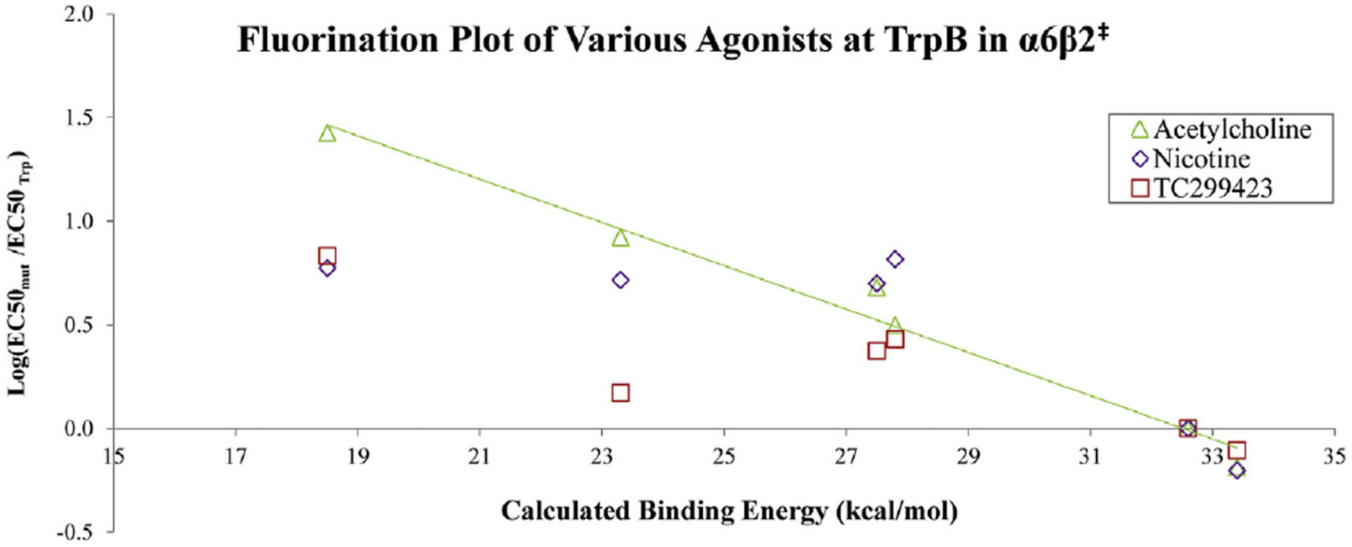

Fig. 6.

Fluorination plot of ACh, nicotine, and TC299423 at TrpB. The trendline is fit to ACh data only. The lack of a linear trend in nicotine and TC299423 indicates these agonists do not make cation-π interactions with the indole side chain.

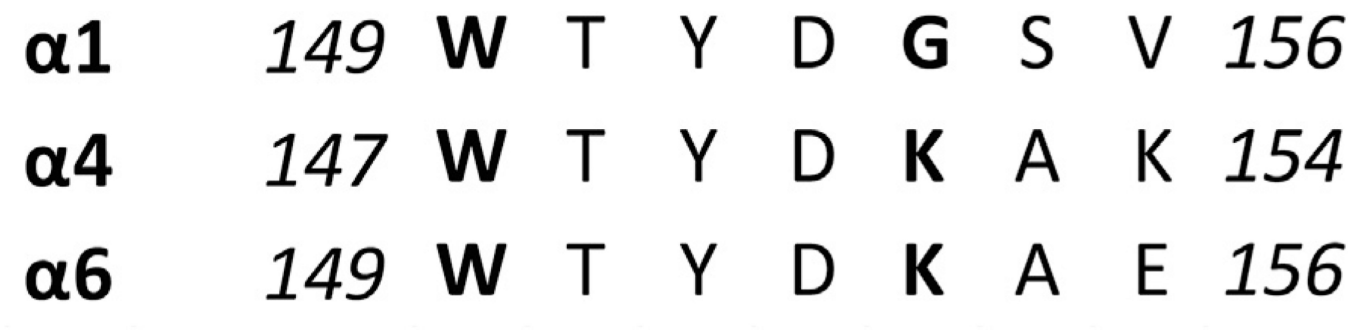

Fig. 7.

Alignment of Loop B in the rat α1, α2, and α6 nAChR subunits. Note the conserved Trp in all three subunits as well as the i + 4 Gly in α1 that aligns with a Lys in α4 and α6.

Table 1

Dose-response relationships for various mRNA α6:β2 injection ratios.

Ratio	EC50 (uM)	n_H	I_{max}	N
50:1	0.097 ± 0.002	1.17 ± 0.03	8.25–57.3	11
20:1	0.139 ± 0.003	1.64 ± 0.05	0.25–1.44	15
10:1	0.119 ± 0.004	1.17 ± 0.04	4.85–70.7	16
5:1	0.094 ± 0.003	1.17 ± 0.04	0.70–79.9	18
2:1	0.109 ± 0.002	1.14 ± 0.03	0.94–79.5	11
1:1	0.15 ± 0.01	1.15 ± 0.06	4.42–14.2	10
1:2	0.125 ± 0.003	1.23 ± 0.05	3.06–31.7	11
1:5	0.35 ± 0.02	0.95 ± 0.04	0.70–8.21	13
1:10	0.80 ± 0.04	0.83 ± 0.02	1.01–4.67	16
1:20	0.52 ± 0.03	0.86 ± 0.03	1.01–10.9	11

Table 2

Agonists at α6β2‡.

	EC50 (μM)	n_H	I_{max} (μA)	N_{EC50}	Eff	N_{Eff}
ACh	0.169 ± 0.003	1.36 ± 0.03	0.28–14.9	12	–	–
Nic	0.057 ± 0.002	1.38 ± 0.05	9.48–54.4	10	0.49 ± 0.03	22
metaNic	0.74 ± 0.02	0.98 ± 0.03	0.43–40.4	13	0.64 ± 0.04	15
Var	0.031 ± 0.003	1.08 ± 0.08	0.51–12.1	15	0.33 ± 0.02	19
Cyt	0.027 ± 0.001	1.31 ± 0.05	0.57–31.9	11	0.28 ± 0.01	20
Ch	159 ± 7	1.32 ± 0.05	2.08–15.4	14	0.33 ± 0.02	15
CCh	1.36 ± 0.05	1.12 ± 0.04	3.63–52.5	13	0.87 ± 0.04	18
Epi	0.00035 ± 0.00003	1.9 ± 0.2	0.47–2.81	12	0.54 ± 0.02	19
TC299	0.071 ± 0.003	0.99 ± 0.04	1.73–21.9	12	0.59 ± 0.04	16

Table 3

Evidence for a cation-π interaction with ACh at 10:1 α6β2[‡].

	EC50 (uM)	n_H	I_{max} uA	Fold	N
Trp	0.169 ± 0.003	1.36 ± 0.03	0.28–14.9	0.94	12
MeTrp	0.110 ± 0.002	1.18 ± 0.02	0.19–19.4	0.61	12
4-F_1Trp	0.210 ± 0.006	1.25 ± 0.04	0.71–6.92	1.17	9
5-F_1Trp	0.81 ± 0.01	1.37 ± 0.03	1.39–14.4	4.50	10
6-F_1Trp	0.66 ± 0.02	1.30 ± 0.04	0.18–4.28	3.67	10
BrTrp	0.53 ± 0.01	1.32 ± 0.04	0.22–15.1	2.94	14
F_2Trp	1.41 ± 0.02	1.43 ± 0.02	0.76–9.33	7.83	9
CNTrp	15.1 ± 0.6	1.25 ± 0.05	0.31–13.3	83.89	14
F_3Trp	4.5 ± 0.2	1.04 ± 0.03	0.09–1.94	25.00	12

Table 4

Lack of evidence for cation-π interactions with nicotine and TC299423 at Trp B in α6β2[‡].

Nic	EC50 (μM)	n_H	I_{max} (μA)	Fold	N
Trp	0.150 ± 0.006	1.43 ± 0.06	0.09–5.8	1	12
MeTrp	0.094 ± 0.003	1.36 ± 0.05	0.31–3.95	0.63	11
F_1Trp	0.75 ± 0.02	1.39 ± 0.06	0.07–2.06	5.00	12
BrTrp	0.98 ± 0.03	1.42 ± 0.04	0.08–5.65	6.53	14
F_2Trp	0.78 ± 0.04	1.30 ± 0.06	0.32–2.13	5.20	10
F_3Trp	0.89 ± 0.02	1.28 ± 0.03	0.05–1.05	5.93	10
TC299423	EC50 (μM)	n_H	I_{max} (μA)	Fold	N
Trp	0.093 ± 0.004	1.09 ± 0.04	0.33–3.78	1	11
MeTrp	0.073 ± 0.004	0.92 ± 0.03	0.15–2.35	0.78	13
F_1Trp	0.22 ± 0.01	1.01 ± 0.04	0.27–3.49	2.37	15
BrTrp	0.25 ± 0.008	1.01 ± 0.03	0.1–7.71	2.69	11
F_2Trp	0.138 ± 0.006	0.98 ± 0.04	0.06–1.87	1.48	11
F_3Trp	0.63 ± 0.03	0.90 ± 0.03	0.05–0.28	6.77	13